Available online at www.sciencedirect.com
SCIENCE DIRECT®
Journal of Organometallic Chemistry 689 (2004) 4856–4867
Journal of Organometallic Chemistry
www.elsevier.com/locate/jorganchem

Ferrocenoyl peptides with sulfur-containing side chains: synthesis, solid state and solution structures

Xavier de Hatten [a], Thomas Weyhermüller [b], Nils Metzler-Nolte [a,*]

[a] Institute for Pharmacy and Molecular Biotechnology, University of Heidelberg, Im Neuenheimer Feld 364, D-69120 Heidelberg, Germany
[b] Max-Planck-Institute for Bioinorganic Chemistry, Stiftstraße 34-36, D-45470 Mülheim/Ruhr, Germany

Received 20 August 2004; accepted 1 October 2004
Available online 5 November 2004

Abstract

The synthesis and full characterization of a number of amino acid and dipeptide derivatives with sulfur-containing side chains derived from ferrocene carboxylic acid and ferrocene-1,1′-dicarboxylic acid is presented. In particular, compounds Fc-CO-$(Aaa)_n$-OMe (**4**) and $Fe[C_5H_4$-CO-$(Aaa)_n$-$OMe]_2$ (**3**) with $(Aaa)_n$ = Cys(Bzl) (**a**), Cys(Bzl)-Cys(Bzl) (**b**), Cys(*p*-OMe-Bzl) (**c**), Cys(*p*-OMe-Bzl)-Cys(*p*-OMe-Bzl) (**d**), Met (**e**), and Met-Met (**f**) were prepared. Also, the free acid derivatives $Fe[C_5H_4$-CO-Met-$OH]_2$ (**6e**) and Fc-CO-Met-OH (**7e**) were prepared and characterized. The solid state structures of **3a**, **4b**, and **4e** were determined by single crystal X-ray diffraction. Compound **3a** shows a 1,3′ substitution pattern on the Cp rings in the solid state. Structures in solution were determined by NMR, IR and CD spectroscopy, with particular emphasis on the question of hydrogen bonding and helical chirality of the metallocene. As an example, the full assignment for the Cp signals in the disubstituted derivative **3a** was achieved by simulation of the ^{1}H NMR signals from the cyclopentadienyl ring in combination with 2D-NOESY spectra. In solution, **3a** has the known 1,2′ substitution pattern, which is stabilized by intramolecular hydrogen bonds.

Keywords: Amino acids; Bioorganometallic chemistry; Ferrocene compounds; Hydrogen bonds; Peptides

1. Introduction

Conjugates of ferrocene and amino acids or peptides have been intensively studied in recent years [1]. The resulting conjugates were investigated as electrochemical sensors for organic substrates [2–5] or anions [6,7]. In addition, such systems may serve as organometallic mimetics of turn structures in peptides as first suggested by Herrick and coworkers [8,9]. We have recently investigated the influence of charge in such systems by replacing ferrocene with the isostructural cobaltocenium cation [10]. Real organometallic turn mimetics with anti-parallel peptide strands can be realized by use of the organometallic amino acid 1′-aminoferrocene-1-carboxylic acid [11–14] as demonstrated in a recent communication [15]. However in most cases studied so far, ferrocene carboxylic acid **1** or ferrocene-1,1′-dicarboxylic acid **2** were coupled to the amino terminus of the biomolecules. In those compounds, the question of structural organization through hydrogen bonds has been investigated in detail in the solid state by X-ray crystallography and IR spectroscopy as well as in solution by IR, NMR and CD spectroscopy [9,16–24,2,25,4,26,27,10,28].

A literature survey reveals that most compounds studied so far were composed of lipophilic amino acids without functional groups in the side chain [29]. These

Abbreviations: Aaa, any amino acid; Bzl, benzyl; Cys, cysteine; EDC, 1-(3-Dimethylaminopropyl)-3-ethylcarbodiimide hydrochloride; HOBt, hydroxy-benzotriazole; IBCF, isobutyl-chloroformate; NMM, *N*-methyl morpholine; Met, methionine; *p*-OMe-Bzl, *p*-methoxybenzyl.

* Corresponding author. Tel.: +6221 54 6442; fax: +6221 54 6441.
E-mail address: nils.metzler-nolte@urz.uni-heidelberg.de (N. Metzler-Nolte).

0022-328X/$ - see front matter © 2004 Elsevier B.V. All rights reserved.
doi:10.1016/j.jorganchem.2004.10.002

compounds are straightforward to prepare and no protecting groups are required. However, it is certainly desirable to provide additional functionality for further derivatization. In this work, we present results on the synthesis and characterization of ferrocenoyl derivatives with sulfur-containing amino acids and dipeptides such as methionine and cysteine.

2. Experimental

2.1. General procedures

CH_2Cl_2 and Et_3N were dried (CaH_2) and distilled under Ar prior to use. MeOH, EtOAc, diethyl ether, hexane, THF, $CDCl_3$, D_2O, CD_3OD (all ACS grade) were used as received. All reactions were carried out under inert gas atmosphere in dried glassware. Amino acids and coupling reagents were obtained from Novabiochem and used without further purification as well as Fc-COOH and Fe(C_5H_4-COOH)$_2$ (Acros). H-Cys(*p*-OMe-Bzl)-OMe was prepared using a standard procedure: H-Cys(*p*-OMe-Bzl)-OH was refluxed in MeOH with $SOCl_2$ overnight. After evaporation of all volatiles, the product was purified by precipitation from cold diethyl ether and dried under reduced pressure to yield an off-white powder that was pure by NMR and used as the crude product. For column chromatography, column were packed with 0.063–0.200 mm silica gel 60 (VWR). For TLC, plates coated with silica gel F_{254} were used. NMR spectra were determined on Brucker AM 360 spectrometer, ^{1}H operating at 360 MHz and ^{13}C operating at 95.56 MHz. 2D spectra were recorded on a Varian Unity 400 spectrometer (^{1}H at 400 MHz) with an inverse probe and *z*-gradients. 2D-NOESY spectra were recorded with 0.5 and 1 s mixing time and compared. Signals in both ^{1}H and ^{13}C are reported in ppm relative to TMS, the internal standard. Spectra of peptides only are referenced to the residual MeOH signal (3.31 ppm ^{1}H, 49.0 ppm ^{13}C). All others compounds are referenced to the TMS signal for ^{1}H or of the residual $CHCl_3$ signal (7.26 ppm ^{1}H, 77.2 ppm) for ^{13}C. Coupling constants, *J*, are given in Hz. Elemental analysis were performed by Foss Heraeus Vario EL Elementar Analysator in C, H, N mode. Infrared spectra were recorded at 20 °C on Brucker Equinox55 FT-IR spectrometer between NaCl windows in distilled $CHCl_3$, or as KBr discs, with a spectral resolution of 2.0 cm^{-1}. Wavenumbers, *v*, are given in cm^{-1}. Mass spectra were measured on a Mat 8200 instrument, EI (70 eV) and FAB (glycerol or NBA matrix), only base peak and characteristic fragments with possible composition are given in brackets. For fragments containing metals only the isotopomer with highest intensity was described. UV/VIS spectra were measured in distilled CH_2Cl_2 on a Varian CARY 100 instrument in 1 cm quartz Suprasil cells thermostated at 25 °C. Absorption maxima, λ_{max}, and molar absorption coefficients, ε, are given in nm and l mol^{-1} cm^{-1}, respectively. Circular dichroism spectra were recorded in distilled CH_2Cl_2, on a JASCO J-810 spectropolarimeter in 1 cm quartz Suprasil cells thermostated at 20 °C under Argon. Cyclic Voltammograms and square wave voltammograms in CH_3CN solutions with NBu_4PF_6 as supporting electrolytes were recorded on a Perkin–Elmer BES Potentiostat/Galvanostat. A three-electrode cell was employed with a glassy carbon working electrode, a platinum-wire auxiliary electrode and a Ag/$AgNO_3$ reference electrode (0.01 M $AgNO_3$ in CH_3CN). For determination of the redox potentials, ferrocene was added as internal standard.

2.2. Preparation of amino acid and dipeptide derivatives

H-Cys(p-OMe-Bzl)-OMe: Yield: 98%. $C_{12}H_{17}NO_3S$, HCl = 291.07 g mol^{-1}. IR (KBr): 3477 (br, ν_{NH}), 3000–2840 (br, ν_{OH} and $\nu_{CH\text{-}Bzl}$), 1744 (s, $\nu_{C=O}$), 1511 (s, $\nu_{NH\text{-}deformation}$). MS(EI): *m/z* = 255 [M$^+$]. ^{1}H NMR (MeOD, 293 K, $c = 10^{-2}$ M): δ 7.25 (2H, m, H_{Ar}), 6.9 (2H, m, H_{Ar}), 3.76–3.74 (3H, s, $CH_{3\text{-}p\text{OMe}}$ and 3H, s, CH_3), 3.65 (1H, m, CH_α), 3.40 (2H, s, CH_2-Bzl), 3.0–2.90 (2H, m, $CH_{2,\beta}$).

Boc-Cys(Bzl)-Cys(Bzl)-OMe: To a stirred solution of Boc-Cys(Bzl)-OH (3.12 g; 10 mmol) in THF (75 mL) was added *N*-methylmorpholine (1.016 g; 1.104 mL; 10 mmol) and isobutyl chloroformiate (1.386 g; 1.320 mL; 10 mmol) resulting in formation of a precipitate. In another flask, H-Cys(Bzl)-OMe, HCl (2.62 mg; 10 mmol) was suspended in THF (50 mL), followed by addition of NEt_3 (1.112 g; 1.386 mL; 10 mmol). The suspensions were mixed, and resulting suspension stirred overnight at ambient temperature, followed by filtration to remove a white precipitate (unreacted materials). The solvent was removed under reduced pressure and the residue dissolved in CH_2Cl_2 (150 mL) and the CH_2Cl_2 solution was washed with distilled water (100 mL) and the phases were separated. The aqueous layer was extracted with CH_2Cl_2 (3 × 70 mL), and the combined organic solutions were dried over $MgSO_4$. Evaporation of the solvent under reduced pressure yielded Boc-Cys(Bzl)-Cys(Bzl)-OMe as a white solid. The product is purified by column chromatography (EtOAc/Hexan (1:2); $R_f = 0.2$). Yield: 4.8 g (93%). $C_{26}H_{34}N_2O_5S_2$ = 518.19 g mol^{-1}. IR (KBr): 3331 (s, ν_{NH}), 3100–2900 (m, br, ν_{OH} and $\nu_{CH\text{-}Bzl}$), 1743 (s, $\nu_{C=O\text{-}ester}$), 1688 (s), 1643 (s, $\nu_{C=O\text{-}amide}$ and $\nu_{C=O\text{-}Boc}$, s), 1511 (s, $\nu_{NH\text{-}deformation}$). MS (EI): *m/z* = 518 [M]$^+$. MS (FAB): *m/z* = 519 [M + H]$^+$, 419 [M − Boc + H]$^+$. ^{1}H NMR ($CDCl_3$, 293 K, $c = 10^{-2}$ M): δ 7.3–7.2 (10H, m, H_{Ar}), 7.23 (1H, d, $^3J_{HH}$ = 7.0, NH), 7.03 (1H, d, $^3J_{HH}$ = 7.5, NH), 4.75 (1H, m, CH_α), 3.92 (1H, m, CH_α), 3.76 (4H, s, $CH_{2,Bzl}$), 3.73 (3H, s, $CH_{3,ester}$), 2.95–2.70 (4H, m, $CH_{2,\beta}$), 1.46 (9H, s, H_{Boc}). ^{13}C NMR ($CDCl_3$, 293

K, $c = 10^{-2}$ M): δ 170.5 ($C{=}O_{ester}$ + $C{=}O_{Boc}$), 137.6 ($C{=}O_{Cys}$), 129.0, 128.9, 128.6, 128.5, 127.3, 127.2 (C_{Ar}), $C_{q,\,Boc}$ is missing, 52.7 (C_α), 51.8 (C_α), 36.6 ($CH_{2\text{-}Bzl}$), 33.3 (C_β), 28.3 ($CH_{3,\,Boc}$).

Boc-Cys(p-OMe-Bzl)-Cys(p-OMe-Bzl)-OMe was prepared via a similar procedure as described for Boc-Cys(Bzl)-Cys(Bzl)-OMe using Boc-Cys(pOMe)-OH (1.4 g; 4.1 mmol) and H-Cys(Bzl)-OMe × HCl (1.050 g; 4.1 mmol). The product was purified by column chromatography (EtOAc/Hexan (1:2); $R_f = 0.2$). Yield: 2.1 g (90%). $C_{28}H_{38}N_2O_7S_2 = 578.21$ g mol^{-1}. FT-IR (KBr): 3329 (s, ν_{amide}), 3100–2900 (m, br, ν_{OH} and $\nu_{CH\text{-}Bzl}$), 1744 (s, $\nu_{C=O,\,ester}$), 1688 (s), 1642 (s, $\nu_{C=O,\,amide}$ and $\nu_{C=O,\,Boc}$), 1511 (s, $\nu_{NH\text{-}deformation}$). MS (EI): $m/z = 578$ $[M]^+$. MS (FAB): $m/z = 579$ $[M + H]^+$, 479 $[M - Boc) + H]^+$. ^{1}H NMR ($CDCl_3$, 293 K, $c = 10^{-2}$ M): δ 7.3–7.2 (8H, m, H_{Ar}), 7.23 (1H, d, $^3J_{HH} = 7.0$, NH), 7.03 (1H, d, $^3J_{HH} = 7.5$, NH), 4.75 (1H, m, CH_α), 3.92 (1H, m, CH_α), 3.76 (4H, s, $CH_{2,\,Bzl}$), 3.73 (3H, s, O–$CH_{3,\,ester}$), 2.95–2.70 (4H, m, $CH_{2,\,\beta}$), 1.46 (9H, s, $CH_{3,\,Boc}$).

2.3. General procedure for the coupling of amino acids or dipeptides with ferrocene mono- or di-carboxylic acid

A stirred suspension of ferrocene carboxylic acid (**1**) (1 mmol; 230 mg) or ferrocene-1-1′-dicarboxylic acid (**2**) (1 mmol; 274 mg) in distilled CH_2Cl_2 (30 mL) was degassed over a period of 15 min. To this suspension were added stoichiometric amounts of HOBt monohydrate (1 mmol; 153.5 mg (**1**), or 2 mmol; 307 mg (**2**)), EDC (1 mmol; 191,7 mg (**1**), or 2 mmol; 383.4 mg (**2**)) and DIPEA (1 mmol; 386 μL (**1**), or 2 mmol; 772 μL (**2**)). The resulting suspension is allowed to stirr at ambient temperature for 30 min. the reaction mixture is then filtered to remove unreacted materials. A stoichiometric amount of corresponding amino acid or dipeptide methyl esters (either 1 or 2 mmol) was added to this solution and stirring is continued at ambient temperature. The disappearance of starting material was followed by TLC using EtOAc/Hexan (1:1). The reaction mixture is then diluted to 100 mL with CH_2Cl_2 and the organic layer is washed consecutively with 50 mL HCl 0.1 M, 50 mL distilled water, 50 mL saturated $NaHCO_3$ and 50 mL distilled water. The organic phase is dried over $MgSO_4$, filtered and the solvent removed under reduced pressure giving the crude orange product.

Fe[C_5H_4-CO-Cys(Bzl)-OMe]$_2$ (**3a**): Chromatographed on silica, EtOAc/hexane (1:1) $R_f = 0.4$. Yield: 75%. $C_{34}H_{36}FeN_2O_6S_2 = 688.14$ g mol^{-1}. Elemental Anal. Calc. for $C_{34}H_{36}FeN_2O_6S_2$: C, 59.30; H, 5.27; N, 4.07, found, C, 59.12; H, 5.36; N, 3.96. MS (EI): $m/z = 688$ $[M]^+$, 564 $[M - Bzl\text{–}OMe]^+$. UV/Vis ($CHCl_3$): 442.4 (254). $E_{1/2} = 448$ mV (vs. Fc/Fc$^+$). FT-IR (KBr): 3273 (s, br, $\nu_{NH,\,amide}$), 3084–2840 (m, ν_{OH} and $\nu_{CH\text{-}Bzl}$), 1745 (s, $\nu_{C=O,\,ester}$), 1627 (s, $\nu_{C=O,\,amide}$), 1540 (s, $\nu_{NH\text{-}deformation}$). FT-IR ($CHCl_3$): 3378 (s, $\nu_{NH,\,amide}$), 3076–2856 (m, br, ν_{OH} and $\nu_{CH\text{-}Bzl}$), 1731 (s, $\nu_{C=O,\,ester}$), 1648 (s, $\nu_{C=O,\,amide}$), 1533 (s, $\nu_{NH\text{-}deformation}$). ^{1}H NMR ($CDCl_3$, 293 K, $c = 10^{-2}$ M): δ 7.54 (2H, d, $J_{HH} = 8.3$, NH), 7.3–7.2 (10H, m, H_{Ar}), 4.99 (2H, m, CH_α), 4.88 (2H, ddd, $J_{HH} = 1.1$, $J_{HH} = 2.5$, $J_{HH} = 2.5$, $H_{Cp,\,ortho}$), 4.72 (2H, ddd, $J_{HH} = 1.1$, $J_{HH} = 2.5$, $J_{HH} = 2.5$, $H_{Cp,\,ortho}$), 4.54 (2H, ddd, $J_{HH} = 1.3$, $J_{HH} = 2.6$, $J_{HH} = 2.6$, $H_{Cp,\,meta}$), 4.39 (2H, ddd, $J_{HH} = 1.3$, $J_{HH} = 2.6$, $J_{HH} = 2.6$, $H_{Cp,\,meta}$), 3.73 (10H, overlapping s, $CH_{3,\,ester}$ and $CH_{2,\,Bzl}$), 2.85 (4H, m, $CH_{2,\,\beta}$). ^{13}C NMR ($CDCl_3$, 293 K, $c = 10^{-2}$ M): δ 172.7 ($C{=}O_{ester}$), 169.3 ($C{=}O_{amide}$), 137.6 ($C_{Ar,\,q}$), 128.0, 127.5, 126.2 (C_{Ar}), 74.8 ($C_{Cp,\,q}$), 71.0, 70.6, 69.7, 69.2 (C_{Cp}), 51.9 and 50.6 (CH_α and $CH_{3,\,ester}$), 35.7 and 31.2 ($CH_{2,\,Bzl}$) and ($CH_{2,\,\beta}$).

Fe[C_5H_4-CO-Cys(Bzl)-Cys(Bzl)-OMe]$_2$ (**3b**): Chromatographed on silica gel (EtOAc/hexane (1:1) $R_f = 0.2$). Yield: 70%. $C_{54}H_{58}FeN_4O_8S_4 = 1074.25$ g mol^{-1}. Elemental Anal. Calc. for $C_{34}H_{36}FeN_2O_6S_2$: C, 60.32; H, 5.44; N, 5.21, found, C, 60.02; H, 5.61; N, 5.19. MS (EI): $m/z = 1074$ $[M]^+$, 630. UV/Vis ($CHCl_3$): 445.2 (402). $E_{1/2} = 387$ mV (vs. Fc/Fc$^+$). FT-IR (KBr): 3275 (s, $\nu_{NH,\,amide}$), 3084–2840 (m, br, ν_{OH} and $\nu_{CH\text{-}Bzl}$), 1745 (s, $\nu_{C=O,\,ester}$), 1627 (s, $\nu_{C=O,\,amide}$), 1541 (s, $\nu_{NH\text{-}deformation}$). FT-IR ($CHCl_3$): 3378 (s, $\nu_{NH,\,amide}$), 3086–2847 (m, br, ν_{OH} and $\nu_{CH\text{-}Bzl}$), 1731 (s, $\nu_{C=O,\,ester}$), 1648 (s, $\nu_{C=O,\,amide}$), 1533 (s, $\nu_{NH\text{-}deformation}$). ^{1}H NMR ($CDCl_3$, 293 K, $c = 10^{-2}$ M): δ 8.21 (2H, d, $^3J_{HH} = 8.0$, NH_{amide}), 7.4–7.2 (20H, m, H_{Ar}), 7.23 (2H, d, $^3J_{HH} = 7.7$, NH_{amide}), 4.84 (2H, m, $H_{Cp,\,o}$), 4.65 (6H, m, 4 CH_α and $H_{Cp,\,ortho}$), 4.45 (2H, m, $H_{Cp,\,meta}$), 4.30 (2H, m, $H_{Cp,\,meta}$), 3.8–3.6 (14H, m, $CH_{2,\,Bzl}$ and CH_3), 2.88–2.69 (8H, m, $CH_{2,\,\beta}$). ^{13}C NMR ($CDCl_3$, 293 K, $c = 10^{-2}$ M): δ 172.7 ($C{=}O_{ester}$), 170.7 ($C{=}O_{amide}$), 170.7 ($C{=}O_{amide}$), 137.7 ($C_{Ar,\,q}$), 137.5 ($C_{Ar,\,q}$), 129.0, 128.7, 127.3 (C_{Ar}), 75.9 ($C_{Cp,\,q}$), 71.8, 71.3, 70.7, 70.1 (C_{Cp}), 52.5 and 52.1 (CH_α and CH_3), 36 and 32.5 ($CH_{2,\,Bzl}$) and ($CH_{2,\,\beta}$).

Fe[C_5H_4-CO-Cys(p-OMe-Bzl)-OMe]$_2$ (**3c**) Chromatographed on silica gel EtOAc/hexane (1:1) $R_f = 0.2$. Yield: 76%. $C_{36}H_{40}FeN_2O_8S_2 = 748.16$ g mol^{-1}. Elemental Anal. Calc. for $C_{34}H_{36}FeN_2O_6S_2$: C, 57.91; H, 5.13; N, 3.75, found, C, 57.67; H, 5.42; N, 3.63. MS (EI): $m/z = 748$ $[M]^+$. UV/Vis ($CHCl_3$): 443.5 (219). $E_{1/2} = 402$ mV (vs. Fc/Fc$^+$). FT-IR (KBr): 3287 (s, $\nu_{NH,\,amide}$), 3085–2835 (m, ν_{OH} and $\nu_{CH\text{-}Bzl}$), 1740 (s, $\nu_{C=O,\,ester}$), 1631 (s, $\nu_{C=O,\,amide}$), 1511 (s, $\nu_{NH\text{-}deformation}$). FT-IR ($CHCl_3$): 3378 (s, $\nu_{NH,\,amide}$), 3002–2838 (m, ν_{OH} and $\nu_{CH\text{-}Bzl}$), 1731 (s, $\nu_{C=O,\,ester}$), 1648 (s, $\nu_{C=O,\,amide\text{-}Fc}$ and $\nu_{C=O,\,amide}$), 1536 (s, $\nu_{NH\text{-}deformation}$). ^{1}H NMR ($CDCl_3$, 293 K, $c = 10^{-2}$ M): 7.55 (2H, d, $^3J_{HH} = 8.0$, NH), 7.2 (4H, m, $H_{Ar,\,o}$), 6.8 (4H, m, $H_{Ar,\,m}$), 4.99 (2H, m, CH_α), 4.88 (2H, s, $H_{Cp,\,o}$), 4.72 (2H, s, $H_{Cp,\,o}$), 4.54 (2H, s, $H_{Cp,\,m}$), 4.39 (2H, s, $H_{Cp,\,m}$), 3.78–3.68 (9H, m,

$CH_{3,pOMe}$ and $CH_{3,ester}$), 3.0–2.80 (8H, m, $CH_{2,Bzl}$ and $CH_{2,\beta}$). ^{13}C NMR ($CDCl_3$, 293 K, $c = 10^{-2}$ M): 173.7 ($C{=}O_{ester}$), 170.3 ($C{=}O_{amide}$), 158.8 ($C_{Ar,C\text{-}OMe}$), 130.0 ($CH_{Ar,m}$), 129.3 ($C_{Ar,C\text{-}CH2}$), 113.6 ($CH_{Ar,o}$), 76.0 ($C_{Cp,q}$), 72.0, 71.6, 70.7, 70.2 (C_{Cp}), 55.2 ($CH_{3,pOMe}$), 52.9 and 51.6 (CH_α and $CH_{3,ester}$), 35.5 and 32.2 ($CH_{2,Bzl}$) and ($CH_{2,\beta}$).

Fe[C_5H_4-CO-Met-OMe]$_2$ (**3e**): Chromatographed on silica gel EtOAc/hexane (9:1) $R_f = 0.4$. Yield: 85%. $C_{24}H_{32}FeN_2O_6S_2 = 564.11$ g mol^{-1}. Elemental Anal. Calc. for $C_{24}H_{32}FeN_2O_6S_2$: C, 51.06; H, 5.71; N, 4.96, found, C, 50.96; H, 5.76; N, 5.08. MS (EI): $m/z = 564$ $[M]^+$. UV/Vis ($CHCl_3$): 443.6 (413). $E_{1/2} = 390$ mV (vs. Fc/Fc^+). FT-IR (KBr): 3306 (s, $\nu_{NH,amide}$), 3085–2844 (m, br, ν_{OH} and $\nu_{CH\text{-}Ar}$), 1739 (s, $\nu_{C=O,ester}$), 1634 (s, $\nu_{C=O,amide}$), 1539 (s, $\nu_{NH\text{-}deformation}$). FT-IR ($CHCl_3$): 3369 (s, $\nu_{NH,amide}$), 3003–2850 (m, br, ν_{OH} and $\nu_{CH\text{-}Ar}$), 1727 (s, $\nu_{C=O,ester}$), 1644 (s, $\nu_{C=O,amide}$), 1537 (s, $\nu_{NH\text{-}deformation}$). ^1H NMR ($CDCl_3$, 293 K, $c = 10^{-2}$ M): 7.8 (2H, d, $^3J_{HH} = 8.75$, NH), 4.95 (4H, m, CH_α and $C_{Ar,o}$), 4.75 (2H, ddd, $J_{HH} = 1.2$, $J_{HH} = 2.44$, $J_{HH} = 2.44$, $H_{Cp,o}$), 4.55 (2H, ddd, $J_{HH} = 1.63$, $J_{HH} = 2.65$, $J_{HH} = 2.65$, $H_{Cp,m}$), 4.35 (2H, ddd, $J_{HH} = 1.63$, $J_{HH} = 2.65$, $J_{HH} = 2.65$, $H_{Cp,m}$), 3.83 (6H, s, CH_3), 2.7 (2H, m, SCH_2), 2.55 (2H, m, SCH_2), 2.15 (2H, m, $CH_{2,\beta}$), 2.11 (6H, s, SCH_3), 1.85 (2H, m, $CH_{2,\beta}$). ^{13}C NMR ($CDCl_3$, 293 K, $c = 10^{-2}$ M): 175.6 ($C{=}O_{ester}$), 170.4 ($C{=}O_{amide}$), 75 ($C_{Cp,q}$), 71.9, 71.4, 70.2, 70.1 (C_{Cp}), 52.9 and 51.3 (CH_α and $CH_{3,ester}$), 30.7 and 30.6 (SCH_2) and ($CH_{2,\beta}$), 15.4 (SCH_3).

Fc-Cys(Bzl)-Cys(Bzl)-OMe (**4b**): Chromatographed on silica (EtOAc/hexane (1:2) $R_f = 0.3$). Yield: 83%. $C_{32}H_{34}FeN_2O_4S_2 = 630.13$ g mol^{-1}. Elemental Anal. Calc. for $C_{34}H_{36}FeN_2O_6S_2$: C, 60.95; H, 5.44; N, 4.44, found, C, 60.68; H, 5.58; N, 4.35. MS (EI): $m/z = 630$ $[M]^+$. UV/Vis ($CHCl_3$): 443.2 (229). $E_{1/2} = 182$ mV (vs. Fc/Fc^+). FT-IR (KBr): 3272 (s, $\nu_{NH,amide}$), 3070–2900 (m, br, ν_{OH} and $\nu_{CH\text{-}Bzl}$), 1747 (s, $\nu_{C=O,ester}$), 1629 (s, $\nu_{C=O,amide}$), 1550 (s, $\nu_{NH\text{-}deformation}$). FT-IR ($CHCl_3$): 3409 (s, $\nu_{NH,amide}$), 3069–2925 (m, ν_{OH} and $\nu_{CH\text{-}Bzl}$), 1746 (s, $\nu_{C=O,ester}$), 1678 (s, $\nu_{C=O,amide\text{-}Fc}$), 1645 (s, $\nu_{C=O,amide}$), 1495 (s, $\nu_{NH\text{-}deformation}$). ^1H NMR ($CDCl_3$, 293 K, $c = 10^{-2}$ M): δ 7.4–7.2 (10H, m, H_{Ar}), 7.12 (1H, d, $^3J_{HH} = 7.4$, NH), 6.55 (1H, d, $^3J_{HH} = 7.0$, NH), 4.78–4.65 (4H, m, H_{Cp} and CH_α), 4.38 (2H, m, H_{Cp}), 4.22 (5H, s, $H_{Cp,unsubstituted}$), 3.86 (2H, m, $CH_{2,Bzl}$), 3.74 (3H, s, CH_3), 3.7 (2H, s, $CH_{2,Bzl}$), 3.0–2.77 (4H, m, $CH_{2,\beta}$). ^{13}C NMR ($CDCl_3$, 293 K, $c = 10^{-2}$ M): δ 177.5 ($C{=}O_{ester}$), 177.6 ($C{=}O_{amide}$), 137.5 ($C_{Ar,q}$), 129.1, 128.9, 128.7, 128.6 (C_{Ar}), 74.9 ($C_{Cp,q}$), 70.8, 69.9, 68.5, 68.1 (C_{Cp}), 52.7 and 52 (CH_α and CH_3), 36.5, 33.7 and 33.1 ($CH_{2,Bzl}$) and ($CH_{2,\beta}$).

Fc-Cys(p-OMe-Bzl)-OMe (**4c**): Chromatographed on silica EtOAc/hexane (1:2) $R_f = 0.3$. Yield: 82%. $C_{23}H_{35}FeNO_4S = 477.16$ g mol^{-1}. Elemental Anal. Calc. for $C_{23}H_{35}FeNO_4S$: C, 57.86; H, 7.39; N, 2.93, found, C, 57.82; H, 7.2; N, 2.89. MS (EI): $m/z = 467$ $[M]^+$, 213 [Fc - CO]$^+$. $E_{1/2} = 240$ mV (vs. Fc/Fc^+). FT-IR (KBr): 3278 (s, $\nu_{NH,amide}$), 3082–2834 (m, br, ν_{OH} and $\nu_{CH\text{-}Bzl}$), 1737 (s, $\nu_{C=O,ester}$), 1628 (s, $\nu_{C=O,amide}$, 1538 (s, $\nu_{NH\text{-}deformation}$). ^1H NMR ($CDCl_3$, 293 K, $c = 10^{-2}$ M): 7.2 (2H, m, $H_{Ar,o}$), 6.8 (2H, m, $H_{Ar,m}$), 6.45 (1H, d, $J_{HH} = 7.34$, NH), 4.95 (1H, m, CH_α), 4.73 and 4.67 (4H, s, H_{Cp}), 4.25 (5H, s, $H_{Cp,unsubstituted}$), 3.78 (5H, s, O-$CH_{3,p\text{-}OMe}$ and $CH_{2,Bzl}$), 3.71 (3H, s, $CH_{3,ester}$), 2.91–2.76 (2H, m, $CH_{2,\beta}$).

Fc-Cys(p-OMe-Bzl)-Cys(p-OMe-Bzl)-OMe (**4d**): Chromatographed on silica (EtOAc/hexane (1:2) $R_f = 0.2$). Yield: 72%. $C_{34}H_{38}FeN_2O_6S_2 = 690.15$ g mol^{-1}. Elemental Anal. Calc. for $C_{34}H_{38}FeN_2O_6S_2$: C, 59.13; H, 5.55; N, 4.06, found, C, 58.94; H, 5.62; N, 3.86. MS (EI): $m/z = 690$ $[M]^+$, 626 $[M - 2\ OMe]^+$. UV/Vis ($CHCl_3$): 441.2 (562). $E_{1/2} = 192$ mV (vs. Fc/Fc^+). FT-IR (KBr): 3278 (s, $\nu_{NH,amide}$), 3083–2900 (m, ν_{OH} and $\nu_{CH\text{-}Bzl}$), 1738 (s, $\nu_{C=O,ester}$), 1628 (s, $\nu_{C=O,amide}$), 1535 (s, $\nu_{NH\text{-}deformation}$). FT-IR ($CHCl_3$): 3434 (s, $\nu_{NH,amide}$), 3015–2976 (m, ν_{OH} and $\nu_{CH\text{-}Bzl}$), 1740 (s, $\nu_{C=O,ester}$), 1653 (s, $\nu_{C=O,amide\text{-}Fc}$), 1609 (s, $\nu_{C=O,amide}$), 1511 (s, $\nu_{NH\text{-}deformation}$). ^1H NMR ($CDCl_3$, 293 K, $c = 10^{-2}$ M): δ 7.2 (4H, m, $H_{Ar,o}$), 6.8 (4H, m, $H_{Ar,m}$), 6.55 (2H, d, $^3J_{HH} = 7.3$, NH), 4.79–4.68 (4H, m, H_{Cp} and CH_α), 4.38 (2H, m, H_{Cp}), 4.22 (5H, s, $H_{Cp,unsubstituted}$), 3.78–3.65 (9H, m, $CH_{3,pOMe}$ and $CH_{3,ester}$), 3.0–2.75 (8H, m, $CH_{2,Bzl}$ and $CH_{2,\beta}$). ^{13}C NMR ($CDCl_3$, 293 K, $c = 10^{-2}$ M): 174.8 ($C{=}O_{ester}$), 170.3 ($C{=}O_{amide}$), 158.8 ($C_{Ar,C\text{-}0Me}$), 130.0 ($CH_{Ar,m}$), 129.3 ($C_{Ar,C\text{-}CH2}$), 113.6 ($CH_{Ar,o}$), 76.3 ($C_{Cp,q}$), 70.8, 69.9, 68.5, 68.1 (C_{Cp}), 55.2 ($CH_{3,pOMe}$), 52.9 and 51.6 (CH_α and $CH_{3,ester}$), 35.5 and 32.2 ($CH_{2,pOMe}$) and ($CH_{2,\beta}$).

Fc-Met-OMe (**4e**): Chromatographed on silica EtOAc/hexane (9:1) $R_f = 0.5$. Yield: 87%. $C_{17}H_{21}FeNO_3S = 375.06$ g mol^{-1}. Elemental Anal. Calc. for $C_{17}H_{21}FeNO_3S$: C, 54.41; H, 5.64; N, 3.73, found, C, 54.14; H, 5.67; N, 3.71. MS (EI): $m/z = 375$ $[M]^+$, 213 $[Fc\text{-}CO]^+$. UV/Vis ($CHCl_3$): 442.7 (211). $E_{1/2} = 190$ mV (vs. Fc/Fc^+). FT-IR (KBr): 3269 (s, $\nu_{NH\text{-}amide}$), 3100–2916 (m, br, ν_{OH} and $\nu_{CH\text{-}Ar}$), 1747 (s, $\nu_{C=O,ester}$), 1625 (s, $\nu_{C=O,amide}$), 1530 (s, $\nu_{NH\text{-}deformation}$). FT-IR ($CHCl_3$): 3432 (s, $\nu_{NH,amide}$), 3100–2849 (m, br, ν_{OH} and $\nu_{CH\text{-}Ar}$), 1738 (s, $\nu_{C=O,ester}$), 1655 (s, $\nu_{C=O,amide}$), 1509 (s, $\nu_{NH\text{-}deformation}$). ^1H NMR ($CDCl_3$, 293 K, $c = 10^{-2}$ M): 6.57 (1H, d, $^3J_{HH} = 7.76$, NH), 4.86 (1H, m, CH_α), 4.75 and 4.9 ($2 \times 1H$, s, H_{Cp}), 4.36 (2H, s, H_{Cp}), 4.24 (5H, s, $H_{Cp,unsubstituted}$), 3.8 (3H, s, $CH_{3,ester}$), 2.6 (2H, t, $^3J_{HH} = 7.2$, SCH_2), 2.2–2.0 (2H, m, $CH_{2,\beta}$), 2.13 (3H, 2, SCH_3). ^{13}C NMR ($CDCl_3$, 293 K, $c = 10^{-2}$ M): 172.6 ($C{=}O_{ester}$), 170.3 ($C{=}O_{amide}$), 75.0 ($C_{Cp,q}$), 70.5, 69.7, 68.4, 68.0 (C_{Cp}), 52 and 51 (CH_α and $CH_{3,ester}$), 31.3 and 30.1 (SCH_2) and ($CH_{2,\beta}$), 15.4 (SCH_3).

2.4. Preparation of Fc-Met-OH 7e and Fe[C_5H_4-CO-Met-OH]$_2$ (6e)

Fc-Met-OMe (**4e**, 2.4 mmol; 895 mg) or Fe[C_5H_4-CO-Met-OMe]$_2$ (**3e**, 1.2 mmol; 676 mg) were dissolved in 40 mL dioxane : water (1:1) and a stoichiometric amount of NaOH (100 mg; 2.4 mmol) was added at 0 °C (ice bath). The mixture was allowed to stirr at 0 °C for 10 min and for an additionnal 60 min at room temperature. Disappearance of the starting material was followed by TLC using EtOAc/hexane (9:1). The solution was acidified with 1 M HCl to pH 1. The aqueous reaction mixture was then extracted with EtOAc (2×70 mL). The organic layer was dried over $MgS0_4$, filtered, and the solvent removed under reduced pressure to yield the orange crude product.

Fc-Met-OH (**7e**) was purified by recrystallisation from cold diethyl ether. Yield: 98%. $C_{16}H_{19}FeNO_3S = 361.04$ g mol^{-1}. Elemental Anal. Calc. for $C_{16}H_{19}FeNO_3S$: C, 53.20; H, 5.30; N, 3.88, found, C, 53.09; H, 5.34; N, 3.55. MS (EI): $m/z = 361$ $[M]^+$, 213 $[Fc\text{-}CO]^+$. UV/Vis ($CHCl_3$): 445.3 (275). FT-IR (KBr): 3260 (s, $\nu_{NH,\,amide}$), 3110–2923 (m, br, ν_{OH} and $\nu_{CH\text{-}Ar}$), 1718 (s, $\nu_{C=O,\,acid}$), 1609 (s, $\nu_{C=O,\,amide}$), 1545 (s, $\nu_{NH\text{-}deformation}$). FT-IR ($CHCl_3$): 3432 (s, $\nu_{NH,\,amide}$), 3089–2836 (m, br, ν_{OH} and $\nu_{CH\text{-}Ar}$), 1731 (s, $\nu_{C=O,\,acid}$), 1652 and 1601 (s, $\nu_{C=O,\,amide}$), 1511 (s, $\nu_{NH\text{-}deformation}$). ^{1}H NMR ($CDCl_3$, 293 K, $c = 10^{-2}$ M): δ 4.84 (1H, m, CH_α), 4.54 (2H, s, H_{Cp}), other signals of substituted Cp ring were obscured by solvent signal around 4.9 ppm, 4.36 (5H, s, $H_{Cp,\,unsubstituted}$), 3.4 (2H, m, SCH_2), 2.74 (2H, m, $CH_{2,\,\beta}$), 2.26 (3H, 2, SCH_3).

Fe[C_5H_4-CO-Met-OH]$_2$ (**6e**) was purified by recrystallisation from cold EtOAc. Yield: 97%. $C_{22}H_{28}FeN_2O_6S_2 = 536.1$ g mol^{-1}. Elemental Anal. Calc. for $C_{22}H_{28}FeN_2O_6S_2$: C, 49.26; H, 5.26; N, 5.22, found, C, 49.24; H, 5.56; N, 4.91. MS (EI): $m/z = 536$ $[M]^+$. FT-IR (KBr): 3338 (s, $\nu_{NH,\,amide}$), 3096–2017 (m, br, ν_{OH} and $\nu_{CH\text{-}Ar}$), 1718 (s, $\nu_{C=O,\,ester}$), 1616 (s, $\nu_{C=O,\,amide}$), 1545 (s, $\nu_{NH\text{-}deformation}$). FT-IR ($CHCl_3$): 3366 (s, $\nu_{NH,\,amide}$), 3003 - 2850 (m, br, ν_{OH} and $\nu_{CH\text{-}Ar}$), 1721 (s, $\nu_{C=O,\,ester}$), 1601 (s, $\nu_{C=O,\,amide}$), 1538 (s, $\nu_{NH\text{-}deformation}$). ^{1}H NMR ($CDCl_3$, 293 K, $c = 10^{-2}$ M): 4.95–4.8 (obscured by solvent signal, m, CH_α and $CH_{Cp,\,o}$), 4.58 (2H, m, Cp_m), 4.47 (2H, m, Cp_m), 2.7 (2H, m, SCH_2), 2.55 (2H, m, SCH_2), 2.15 (2H, m, $CH_{2,\,\beta}$), 2.09 (6H, s, SCH_3), 1.91 (2H, m, $CH_{2,\,\beta}$).

2.5. Preparation of Fe[C_5H_4-CO-Met-Met-OMe]$_2$ (3f) and Fc-Met-Met-OMe (4f)

To a stirred solution of either Fc-Met-OH (722 mg; 2 mmol) or Fc-(Met-OH)$_2$ (536 mg; 1 mmol), in THF (20 mL) was added N-methylmorpholine (203 mg; 221 μL; 2 mmol) and isobutyl chloroformiate (277 mg; 264 μL; 2 mmol) resulting in formation of a precipitate. In another flask, H-Met-OMe × HCl (400 mg; 2 mmol) was suspended in THF (20 mL), followed by addition of NEt_3 (222 mg; 277 μL; 2 mmol). The suspensions were mixed, and resulting suspension stirred overnight at ambient temperature, followed by filtration to remove a white precipitate (unreacted materials). The solvent was removed under reduced pressure, the residue dissolved in CH_2Cl_2 (100 mL) and the CH_2Cl_2 solution was washed with distilled water (70 mL) and the phases were separated. The aqueous layer was extracted with CH_2Cl_2 (3×30 mL), and the combined organic solutions were dried over $MgSO_4$. Evaporation of the solvent under reduced pressure yielded either Fc-Met-Met-OMe (**4f**) or Fc-(Met-Met-OMe)$_2$ (**3f**) as orange solid.

Fe[C_5H_4-CO-Met-Met-OMe]$_2$ (**3f**): Chromatographed on silica. Yield: 67%. $C_{34}H_{50}FeN_4O_8S_4 = 826.19$ g mol^{-1}. MS (EI): $m/z = 564$ $[M]^+$. UV/Vis ($CHCl_3$): 448. FT-IR (KBr): 3279 (s, $\nu_{NH,\,amide}$), 3082–2918 (m, br, ν_{OH} and $\nu_{CH\text{-}Ar}$), 1744 (s, $\nu_{C=O,\,ester}$), 1628 (s, $\nu_{C=O,\,amide}$), 1545 (s, $\nu_{NH\text{-}deformation}$). FT-IR ($CHCl_3$): 3416–3316 (two s, $\nu_{NH,\,amide}$), 3034–2878 (m, br, ν_{OH} and $\nu_{CH\text{-}Ar}$), 1741 (s, $\nu_{C=O,\,ester}$, 1640 (s, $\nu_{C=O,\,amide}$), 1529 (s, $\nu_{NH\text{-}deformation}$). ^{1}H NMR ($CDCl_3$, 293 K, c = 10^{-2} M): δ 8.55 (2H, d, $J_{HH} = 8.75$, NH), 7.8 (2H, d, $J_{HH} = 6.0$, NH), 4.8 (8H, m, 4 CH_α and 2 $H_{Cp,\,o}$), 4.52 (2H, s, $H_{Cp,\,m}$), 4.29 (2H, s, $H_{Cp,\,m}$), 3.74 (6H, s, $CH_{3,\,ester}$), 2.6 (8H, m, SCH_2), 2.28–1.92 (20H, m, 4 SCH_3 and 4 $CH_{2,\,\beta}$). ^{13}C NMR ($CDCl_3$, 293 K, $c = 10^{-2}$ M): δ 174.3 ($C{=}O_{ester}$), 172.1 ($C{=}O_{amide}$), 170.7 ($C{=}O_{amide}$), 75.5 ($C_{Cp,\,q}$), 71.8, 71.2, 70.1, 70.0 (C_{Cp}), 52.8, 52.4 and 51.8 (2 C_α and $CH_{3,\,ester}$), 31.3 and 30.6 (SCH_2 and $CH_{2,\,\beta}$), 15.1 (6H, s, SCH_3).

Fc-Met-Met-OMe (**4f**): Chromatographed on silica. Yield: 86%. $C_{34}H_{50}FeN_4O_8S_4 = 516.18$ g mol^{-1}. MS (EI): $m/z = 596$ $[M + 90]^+$. UV/Vis ($CHCl_3$): 445. FT-IR (KBr): 3267 (s, $\nu_{NH,\,amide}$), 3075–2954 (m, br, ν_{OH} and $\nu_{CH\text{-}Ar}$), 1744 (s, $\nu_{C=O,\,ester}$), 1628 (s, $\nu_{C=O,\,amide}$), 1545 (s, $\nu_{NH\text{-}deformation}$). FT-IR ($CHCl_3$): 3416–3316 (two s $\nu_{NH\text{-}amide}$), 3033–2879 (m, br, ν_{OH} and $\nu_{CH\text{-}Ar}$), 1741 (s, $\nu_{C=O,\,ester}$), 1647 (s, $\nu_{C=O,\,amide}$), 1534(s, $\nu_{NH\text{-}deformation}$). ^{1}H NMR ($CDCl_3$, 293 K, $c = 10^{-2}$ M): 7.2 (obscured by solvent signal, NH), 4.8–4.75 (2H, m, CH_α), 4.52–4.2 (9H, H_{Cp}), 4.0 (3H, s, $CH_{3,\,methyl}$), 2.1–1.95 (8H, m, 2 SCH_2 and 2 $CH_{2,\,\beta}$), 1.5 (6H, m, SCH_3).

2.6. X-ray crystallography

Suitable crystals of **3a** were obtained by slow diffusion of pentane into a ethyl acetate solution. Single crystals of **4b** and **4e** were obtained by slow evaporation of CH_2Cl_2/heptane solutions of the compounds. The crystals were coated with perfluoropolyether, picked up with a glass fiber and mounted in the nitrogen cold stream of a Bruker–Nonius Kappa-CCD diffractometer. Intensity data were collected at 100 K using graphite monochromated Mo K_α radiation

($\lambda = 0.71073$ Å) of rotating anode setup. Final cell constants were obtained from least squares fit of a subset of several thousand strong reflections. Data collection was performed by hemisphere runs taking frames at 1.5°, for **3a** and **4b**, and 1.0° in ω for **4e**. Crystal faces were indexed and the Gaussian type absorption correction routine embedded in XPREP was used to correct for absorption. The SHELXTL software package [30] was used for solution and artwork of the structures. Refinement was performed with SHELX97 [31]. The structures were readily solved by direct methods and difference Fourier techniques. Absolute structure parameters were checked by refining the inverse structure and are reliable. All non-hydrogen atoms were refined anisotropically. Hydrogen atoms bound to carbon were placed at calculated positions and refined as riding atoms with isotropic displacement parameters. Hydrogen atoms bound to amide nitrogens were located from the difference map and were isotropically refined with a displacement parameter being 1.2 times the value of Ueq of the amide nitrogen atom. Crystallographic data of the compounds are tabulated in Table 1. CCDC 248033 – 248035 (**3a**, **4b**, and **4e**) contain the supplementary crystallographic data for this paper. These data can be obtained free of charge at www.ccdc.cam.ac.uk/conts/retrieving.html or from the Cambridge Crystallographic Data Centre, 12 Union Road, Cambridge CB2 1EZ, UK; Fax: (internat.) ++44-1223-336-033; E-mail: deposit@ccdc.cam.ac.uk.

3. Results

3.1. Synthesis and characterization

The ferrocene amino acid conjugates were prepared according to Scheme 1. Ferrocene-1,1′-dicarboxylic acid (**1**) or ferrocene carboxylic acid (**2**) were activated with EDC and HOBt. Subsequent addition of either Met or Cys amino acid ester yields the amino acid conjugates **3** and **4**, respectively. Enantiomericall pure L amino acids were used in all cases. The sulfur groups of the cysteine derivatives were protected by benzyl (Bzl) or *p*-methoxy-benzyl (*p*-OMe-Bzl) groups. Dipeptide conjugates **3b**, **d** and **4b**, **d** were obtained after addition of the dipeptides H-Cys(Bzl)-Cys(Bzl)-OMe **5b** or H-Cys(*p*-OMe-Bzl)-Cys(*p*-OMe-Bzl)-OMe **5d**. This synthesis scheme did not work satisfactorily for the methionine dipeptides **3**, **4f**. Instead, the methyl ester in ferrocene-methionine conjugates **3e** and **4e** were hydrolyzed to yield the free acids $Fe[C_5H_4\text{-}CO\text{-}Met\text{-}OH]_2$ (**6e**) and Fc-CO-Met-OH (**7e**). Activation of the acid and coupling to H-Met-OMe yielded the desired methionine dipeptides **3f** and **4f** in good yield. All compounds **3** and **4** were purified by column chromatography on silica. Recrystallization yielded orange crystals, which were suitable for X-ray crystal determination in the case of **3a**, **4b**, and **4e**.

All new compounds were comprehensively characterized. The orange colour is attributed to an absorption in the visible region around 445 nm. Electron ionization

Table 1
Summary of crystallographic data for **3a**, **4b**, and **4e**

	3a	**4b**	**4e**
Chemical formula	$C_{34}H_{36}FeN_2O_6S_2$	$C_{32}H_{34}FeN_2O_4S_2$	$C_{17}H_{21}FeNO_3S$
Fw	688.62	630.58	375.26
Crystal size (mm)	$0.10 \times 0.06 \times 0.02$	$0.24 \times 0.12 \times 0.04$	$0.163 \times 0.050 \times 0.045$
Crystal system	Monoclinic	Tetragonal	Orthorhombic
Space group	$P2_1$ (No. 4)	$P4_3$ (No. 78)	$P2_12_12_1$ (No. 19)
Unit cell dimensions			
a (Å)	9.7500(6)	13.5835(3)	10.5221(3)
b (Å)	12.4980(9)	13.5835(3)	16.5013(4)
c (Å)	13.9735(9)	16.6873(4)	19.6449(6)(12)
β (°)	105.74(1)	90	90
V (Å^3)	1638.90(19)	3079.00(12)	3410.91(16)
Z	2	4	8
D_{calc} (g/cm^3)	1.395	1.360	1.462
Temperature (K)	100(2)	100(2)	100(2)
$2\theta_{max}$ °/total number of reflections collected	62.14/42167	62/81349	62.08/82966
Absolute coefficient (mm^{-1})	0.635	0.664	1.020
R_1 ($I>2\sigma(I)$)[a]	0.0352	0.0304	0.0385
wR_2 (all data)[b]	0.0757	0.0720	0.0744
Data/restraints/parameters	10,397/1/406	9800/2/377	10,885/1/425
Goodness-of-fit on F^2[c]	1.035	1.071	1.040
Min/Max residual density (e Å^{-3})	0.519/−0.291	0.293/−0.202	0.471/−0.382
Flack parameter	−0.003(8)	0.001(7)	0.000(9)

[a] $R_1 = \sum||F_o| - |F_c||/\sum|F_o|$.
[b] $wR_2 = [\sum[w(F_o^2 - F_c^2)^2]/\sum[w(F_o^2)_2]^{1/2}$, where $w = 1/\sigma^2(F_o^2) + (aP)^2 + bP$, $P = (F_o^2 + 2F_c^2)/3$.
[c] Goodness-of-fit $= [\sum[w(F_o^2 - F_c^2)^2]/(n-p)]^{1/2}$, where n = number of reflections and p = number of refined parameters.

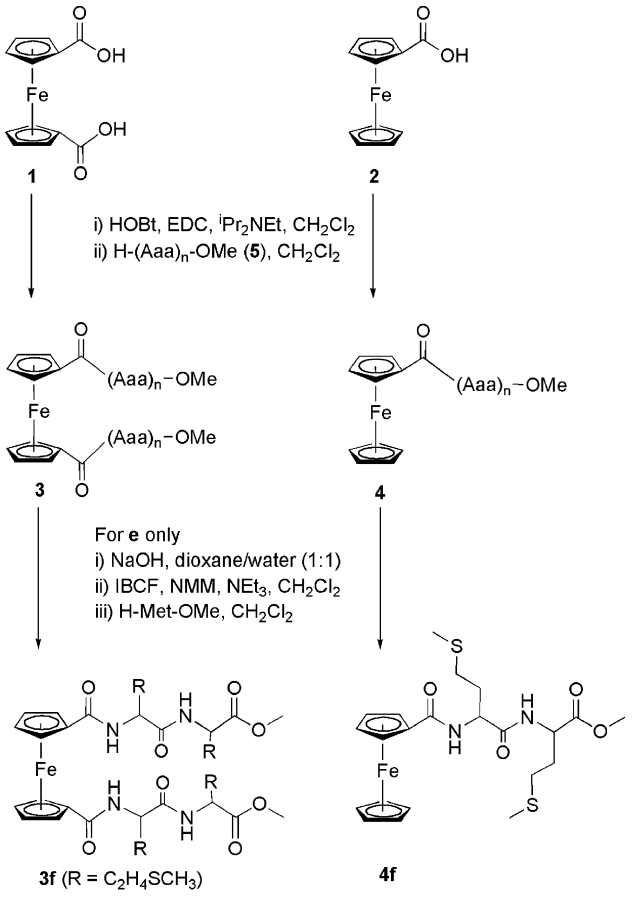

Scheme 1. Synthesis of ferrocenoyl amino acid and peptide derivatives.

(EI) mass spectrometry clearly confirms the composition of all new compounds. Indeed, the M^+ peak is one of the strongest signals in many compounds. Naturally, the dipeptide conjugates with higher mass were less volatile and therefore, the M^+ peak is lower in intensity, although still clearly detectable.

All compounds show a reversible one-electron oxidation for the ferrocene moiety in solution. The oxidation potential for the mono-substituted derivatives **4** is at about 200 mV vs. Fc/Fc^+, whereas it appears at around 400 mV in the disubstituted derivatives **3**. There is a maximum difference of 50 mV between the various amino acids. However, no clear trend is discernible from our data.

NMR spectroscopy also confirms the composition of the compounds even at first glance. All signals for the amino acid side chains are readily assigned by 2D spectroscopy or comparison to literature values. Ester hydrolysis (in **6**, **7e**) is evident from the disappearance

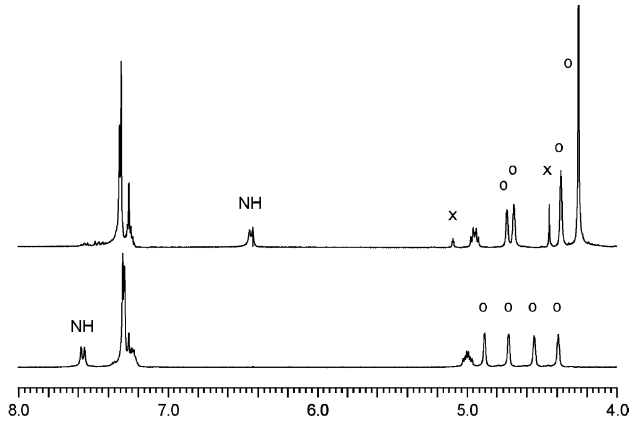

Fig. 1. NMR spectra of **4a** (top) and **3a** (bottom), Cp and aromatic/amide region only. Cp signals are marked with "o", "x" denotes an impurity.

of the singlet for the methyl ester at about 3.8 ppm. The amide protons appear between 7.0 and 8.5 ppm in $CDCl_3$ solution as a doublet due to coupling with the C_α proton. Their position is indicative for the presence or absence of hydrogen bonding, as will be discussed below. The ferrocene groups show characteristic patterns between 4 and 4.5 ppm in all compounds (Fig. 1). Signals with intensity 5:2:1:1 H are observed for the mono-substituted ferrocene derivatives **4**. In contrast, the diacid derivatives **3** show four signals between 4.2 and 4.4 ppm. In some cases, the coupling pattern was very well resolved. For compound **3a**, we were able to extract all coupling constants by simulation of the spectrum (Fig. 2). The assignment of all four signals was possible in combination with a 2D-NOESY spectrum and is discussed below.

3.2. Solid state structures

Single crystals suitable for X-ray analysis were obtained by slow diffusion of pentane in a solution of ethyl acetate for **3a**. Single crystal for both **4b** and **4e** were

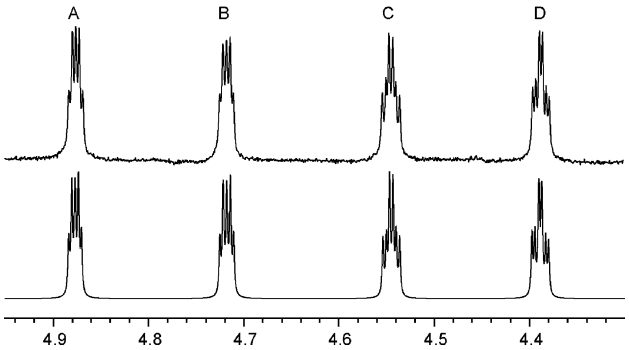

Fig. 2. Cp region of the NMR spectrum of **3a** (top) and simulation (bottom). The following parameters were used in the simulation: $\delta_A = 4.88$; $\delta_B = 4.72$; $\delta_C = 4.54$; $\delta_D = 4.39$; $J_{AB} = 1.2$ Hz; $J_{AC} = 2.5$ Hz; $J_{BC} = 1.3$ Hz; $J_{AD} = 1.1$ Hz; $J_{BD} = 2.7$ Hz; $J_{CD} = 2.5$ Hz. See discussion for assignment of signals.

obtained by slow evaporation of CH_2Cl_2 from a CH_2Cl_2/heptane mixture. In order to determine the conformation and possible hydrogen bonding interactions, the X-ray single crystal structures of those derivatives were determined (see Table 1 for experimental details). All compounds crystallize in chiral space groups as expected and frequently observed before for metallocene amino acid derivatives [9,32,33]. ORTEP plots are shown in Figs. 3–5.

All structures confirm the proposed composition of the compounds. None of the compounds shows any intramolecular hydrogen bonding. However, all amide protons are engaged in intermolecular hydrogen bonding. In compound **4e**, only one amide bond per molecule is present, and this leads to extended chains in the solid state through hydrogen bonding between the amide proton and the carbonyl oxygen atom of the amide group of the neighbouring molecule (N(7)H–O(26) and N(27)H–O(6A)). For both other compounds, several amide bonds are present and a more complicated intermolecular hydrogen bonding pattern is observed which is not further discussed in this article. It is noteworthy that the disubstituted derivative **3a** shows a 1,3′ substitution pattern of the ferrocene moiety. Consequently, the distance between the two Cys residues is too large for intramolecular hydrogen bonding.

3.3. Structures in solution

Although solid state structures provide reliable and accurate data about the molecular constitution, they may not be representative for the structure in solution.

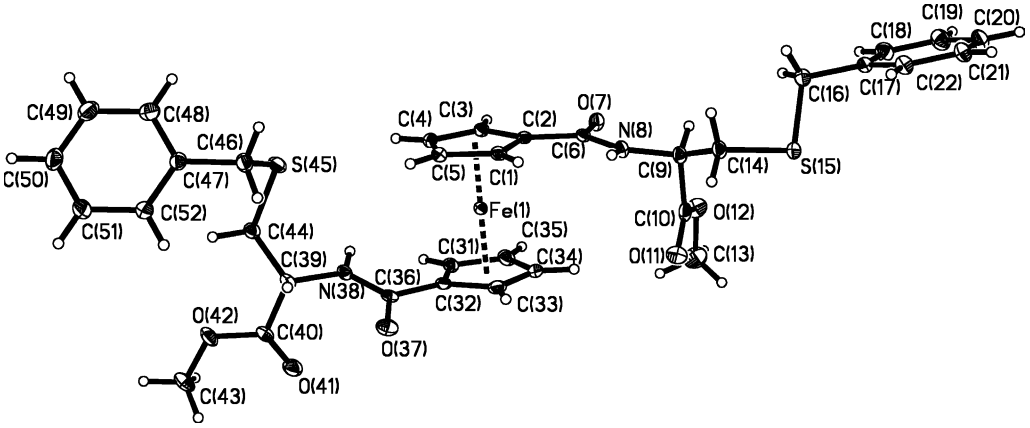

Fig. 3. ORTEP plot of **3a**. Thermal ellipsoids are depicted at 50% probability.

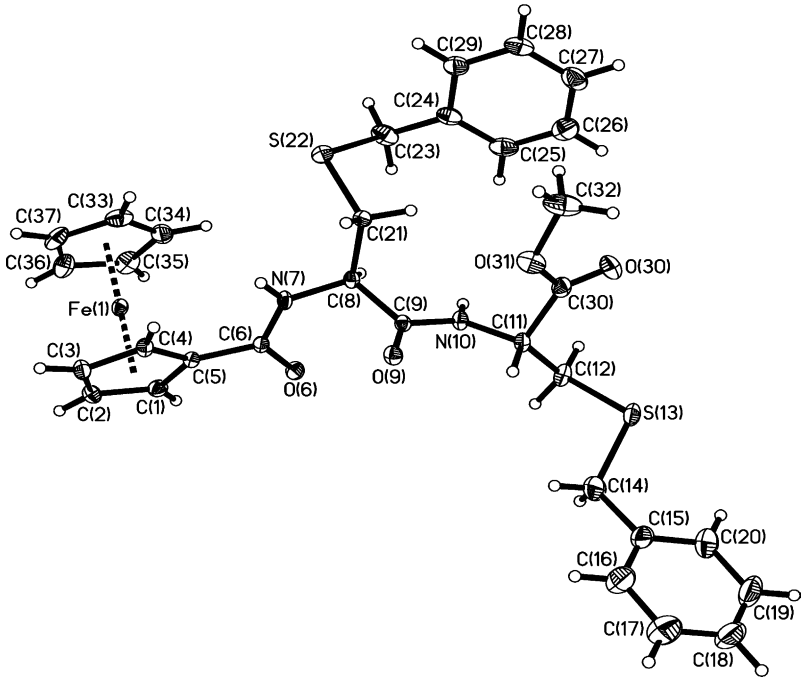

Fig. 4. ORTEP plot of **4b**. Thermal ellipsoids are depicted at 50% probability.

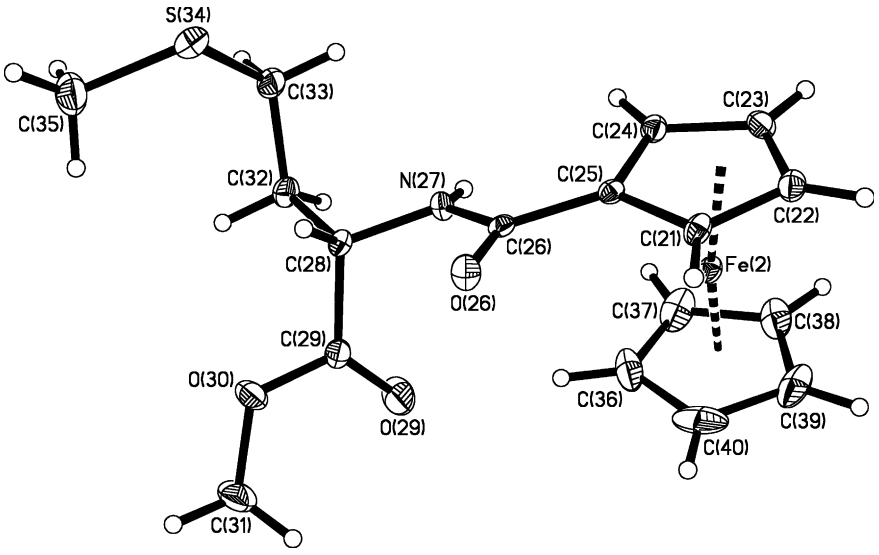

Fig. 5. ORTEP plot of **4e**. Only one of the two independent molecules in the unit cell is shown. Thermal ellipsoids are depicted at 50% probability.

Several methods can be used to obtain information of the structures in solution, in particular about the hydrogen bonding pattern. Methods that were used previously include IR spectrosocopy in the solid state and solution, [34,35,9,2,10] NMR spectroscopy [10,36] and CD spectroscopy [21,15].

Some pertinent data from IR and NMR spectroscopy are tabulated in Table 2. From the IR spectra, we have extracted the NH stretching vibration, the amide carbonyl stretching vibration and the amide bending mode. The latter two are also frequently referred to as "amide I" and "amide II". These bands are among the strongest absorptions in the spectra, along with the ester carbonyl stretching vibration at around 1730 cm^{-1}.

We have also recorded CD spectra of compounds **3** and **4**. Two representative examples are depicted in Fig. 6. Spectra were recorded in $CHCl_3$ at concentrations of about 3.2 mM (**4e**, spectra B) and 0.15 mM (**3e**, spectrum A), respectively. The concentration for **3e** was chosen ten times lower than for **4e** in order to display both spectra on the same absolute ellipticity scale in Fig. 6. Naturally, molar ellipticity coefficients are much higher for **3e** than for **4e** [37]. Metal-centred transitions are expected in the region above 400 nm. For the disubstituted derivatives **3**, a strong positive Cotton effect is seen around 480 nm (**3e**: $M_\theta = 38{,}950\ l\ mol^{-1}\ cm^{-1}$ at 485 nm). A 100-fold weaker positive band is seen for the mono-substituted derivatives **4** around 460 nm (**4e**: $M_\theta = 402\ l\ mol^{-1}\ cm^{-1}$ at 460 nm), followed by a weak negative band around 500 nm (**4e**: $M_\theta = -1610\ l\ mol^{-1}\ cm^{-1}$ at 500 nm). A spectrum of **4e** was also recorded in $CHCl_3$/MeOH (9:1) in order to clarify whether the ferrocene-based bands above 400 nm in compounds **4** originate from inter- or intramolecular hydrogen bonding interactions (spectrum C, 3.2 mM). In the region below 400 nm, which is mainly attributed to transitions of the amino acids, all spectra are rather comparable.

4. Discussion

The synthesis of mono- and disubstituted amino acid and peptide derivatives of ferrocene carboxylic acid **1** and ferrocene 1,1′-dicarboxylic acid **2** proceeds without problems. Coupling of the dipeptide is possible as well as two sequential couplings. The preferred sequence is obviously dependent on the nature of the amino acids and in fact mostly dictated by preparative aspects such as ease of purification. In our hands, the Met–Met dipeptide derivatives **3f** and **4f** were best prepared in the latter fashion, whereas the Cys-containing peptides **b** and **d** were most easily obtained by direct coupling of the dipeptide. The Cys derivatives **a/b** and **c/d** only differ slightly in the protecting group (benzyl vs. *p*-methoxy-benzyl) and are indeed almost identical in their chemical and spectroscopic properties. Therefore, not all possible *p*-methoxy-benzyl derivatives were fully investigated. Most compounds in this study are crystalline solids and as such easily obtained in high purity. Full characterization is possible, and all analytical data corroborate the proposed composition of the compounds. Compound **4a** has been previously prepared by Kraatz and coworkers [23]. This group has also reported sulfur-containing ferrocene derivatives, although not with amino acid but cystamine substitutents [38,39]. Finally, a chinese group has recently reported the synthesis of the S-ethyl protected derivative $Fe[C_5H_4\text{-}CO\text{-}Cys(SEt)\text{-}OMe]_2$ [40,41]. Unlike in this derivative, the Cys protecting groups that were chosen in this work may be removed under reductive conditions.

Table 2
Summary of selected IR and NMR spectroscopic data for compounds **3** and **4**

Compound	ν(NH valence)[a]	ν(C=O valence)[a]	ν(NH deformation)[a]	ν(NH valence)[b]	ν(C=O valence)[b]	ν(NH deformation)[b]	δ_{NH} [c]	$^3J_{HH}$ [d]
4a [23]	Not reported	Not reported	Not reported	Not reported	Not reported	Not reported	6.47*	7.0
3a	3273	1627	1540	3378	1648	1533	7.54	8.3
3b	3275	1628	1541	3378	1648	1541	8.21/7.23	8.0/7.7
3c	3287	1631	1511	3378	1648	1536	7.55	8.0
3e	3306	1634	1539	3369	1644	1537	7.8	8.7
3f	3279	1628	1545	3416/3316	1640/1673	1529	8.55/7.8	8.75/6.0
6e	3338	1616	1545	3366	1601	1538	n.d.[e]	n.d.[e]
4b	3272	1629	1550	3409	1678	1495	7.12/6.55	7.4/7.0
4d	3278	1628	1535	3434	1658	1511	6.55	7.3
4e	3269	1625	1530	3432	1655	1509	6.57	7.7
7e	3260	1609	1545	3432	1652/1601	1511	n.d.[e]	n.d.[e]

[a] As KBr disks.
[b] In cm^{-1}, in dry $CDCl_3$.
[c] In ppm.
[d] In Hz.
[e] Could not be determined because the compounds were only soluble in protic solvents such as CD_3OD where rapid H–D exchange occurs.

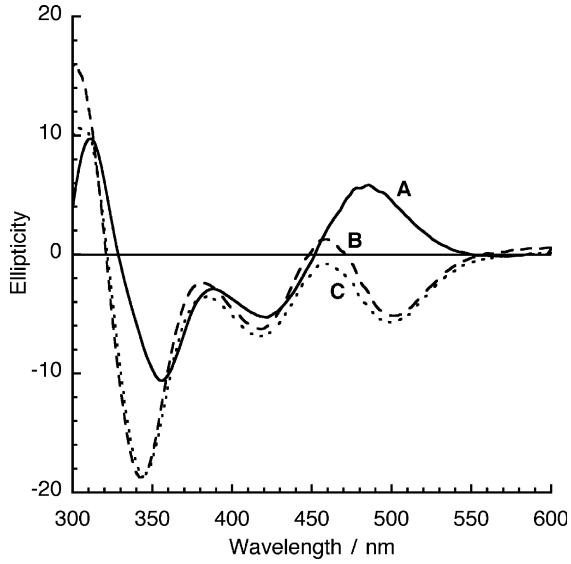

Fig. 6. CD spectra of **3e** (A, conc. is 0.15 mM in $CHCl_3$) and **4e** (B, conc. is 3.2 mM in $CHCl_3$) and **4e** (C, conc. is 3.2 mM in $CHCl_3$: MeOH, 9:1). Please note the different concentrations for **4e** and **3e**, see Section 3.3 for discussion.

Depending on solvent and sample concentration, broad signals in the ^1H NMR spectra are observed for some compounds in $CDCl_3$ solution. This may be due to intermolecular interactions in solution through hydrogen bonding, especially in higher concentrations for the dipeptide derivatives of **1**, like **4b** and **4f**. On the other hand, some of the derivatives **3** do indeed show extremely well-resolved ^1H NMR spectra. By manual iterative simulation, we were able to extract all coupling constants for one derivative as shown in Fig. 2 (see legend of Fig. 2 for values). In combination with 2D-NOESY spectra, we were able to assign signals A–D as shown in Scheme 2, assuming a 1,2′ conformation of the substitutents in solution (see below for discussion of this point). The two signals A and B at lower field are both *ortho* to the amide substituent, as deduced from their chemical shift and coupling constant pattern. A strong NOE is observed between the Cp amide proton and proton B, which is therefore assigend as shown in Scheme 2. From there, coupling constants suggest the order of protons given in Scheme 2, which is also supported by the 2D NMR data.

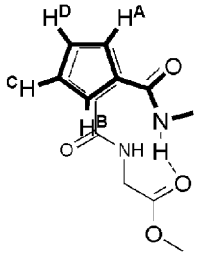

Scheme 2.

One important feature of ferrocenoyl amino acid ester conjugates is the conformation of disubstituted derivatives such as compounds **3a**, **c**, and **e** in this study. The question of hydrogen bonding can be elucidated by a variety of techniques. Some interesting data are summarized in Table 2. It is well established that NH stretching vibrations below 3400 cm^{-1} indicate hydrogen bonding of the amide proton [35,34]. In solution, this is the case for all disubstituted compounds **3**. For monosubstituted derivatives **4**, the intermolecular hydrogen bonds which exist in the solid state are broken up in solution and values above 3400 cm^{-1} are observed for this class of compounds. For the bis(dipeptide) derivative **3f**, two bands are observed which are assigned to the two amide bonds, one which is engaged in hydrogen bonding (probably the one on the Cp ring), and the other which is not. It is surprising, however, that compound **3b** shows only one NH band. This seems to suggest that also the other amide proton is engaged in a hydrogen bond. Kraatz et al. have also discussed the significance of other IR bands in relation to amide hydrogen bonding. In this study, twelve different derivatives are listed in Table 2. From those data, it is evident that only the NH deformation (''amide II'') in solution is of any diagnostic value, in that a shift of 30 cm^{-1} to higher wavenumbers indicates hydrogen bonding. Values around 1540 cm^{-1} do indeed correlate with hydrogen bonding, whereas in non-hydrogen bonded derivatives values of 1500–1510 cm^{-1} are observed.

A second criterium for hydrogen bonding is a significant downfield shift of the amide proton in the ^1H NMR spectrum of about 1 ppm [42]. This is confirmed for all compounds in this study. Indeed, two amide resonances at 7.12 and 6.55 ppm are observed for **3b**, suggesting two different amide protons with and without hydrogen bonding. A value of $^3J_{H\alpha-NH}$ coupling constants >8 Hz is also indicative for hydrogen bonding, although this is not a stringent criterium.

In most disubstituted compounds studied so far, a 1,2′ substitution pattern of the Cp rings was observed. This conformation is stabilized by hydrogen bonds between the two amino acid esters involving the Cp amide hydrogen atom and the carbonyl oxygen atom of the ester group (''Herrick conformation'') [8]. In all those cases, alanine was the first amino acid on the Cp ring. We have recently observed a different hydrogen bonding pattern in the bulkier phenylalanine derivative $Fe[C_5H_4$-CO-Phe-OMe$]_2$ **3g**, involving the amide hydrogen of one Cp ring and the amide carbonyl oxygen atom of the other Cp ring in the same molecule (''van Staveren conformation'') [10]. This second conformation is more strained in that the amide groups need to turn towards each other in a smaller ring. By careful analysis of the spectroscopic data in solution, however, it was shown that **3g** also assumed a ''Herrick conformation'' in solution.

For compound **3a** in this study, the situation is again different. This compound has a 1,3′ conformation in the solid state, and therefore does not show any intramolecular hydrogen bonding in the solid state. All spectroscopic data, however, are similar to previously reported data and thus a 1,2′ conformation with ''Herrick-like'' intramolecular hydrogen bonding is likely. This hydrogen bonding interaction is very strong indeed. CD spectra of **3a** look exactly the same in $CHCl_3$ and in pure MeOH which may compete for hydrogen bonds. In particular, the strong positive Cotton effect at 480 nm is maintained in both solvents. One might argue that the 1,3′ conformation in the solid state is due to steric interactions of the bulky Cys(Bzl) side chains. However, a 1,3′ conformation in the solid state has also been observed for the glycine ethyl ester derivative $Fe[C_5H_4$-CO-Gly-OEt$]_2$ by Kraatz and coworkers. In fact, the related free acid $Fe[C_5H_4$-CO-Gly-OH$]_2$ shows the well-known 1,2′ ''Herrick conformation'' in the solid state [43]. It seems therefore reasonable to summarize that the factors governing the solid state structures are not yet fully understood.

Finally, our CD spectroscopic measurements correlate nicely with results from Hirao and coworkers [22,21]. A positive Cotton effect at 480 nm is indicative for a *P*-helical arrangement of the substituents on the Cp rings in disubstituted compounds **3** (Fig. 6, spectrum A). A similar conclusion was also drawn for a tetrapeptide containing the unnatural amino acid 1-aminoferrocene-1′-carboxylic acid [15]. It is interesting to note that also the monosubstituted derivatives **4** show an appreciable CD signal above 400 nm. It is, however, much weaker than in derivatives **3**, and has a different appearance as shown in Fig. 6 for **4e** (spectrum B, note that spectrum A was recorded at a 10 times lower concentration, molar ellipticity values are given in Section 3.3 above). One might argue that this signal is due to the proximity of the chiral centre (C_α) on one Cp ring, which induces a polarization in the metal-centred d-d or metal-to-ligand transitions and thus a CD signal at low wavelength. Alternatively, it might be due to intermolecular hydrogen bonding interactions. To test this hypothesis, we have added 10% MeOH to the solution of **4e** in $CHCl_3$ (spectrum C, Fig. 6). Spectra B and C look very similar. Therefore, we conclude that the observed CD bands above 400 nm are an intrinsic property of a single molecule and not due to intermolecular hydrogen bonding interactions.

5. Conclusions

We have carried out a comprehensive study on ferrocenoyl derivatives with sulfur containing amino acids and dipeptides. Almost all possible combinations of ferrocene carboxylic acid and ferrocene-1,1′-dicarboxylic

acid with methionine and two differently protected cysteine methyl ester derivatives were prepared as mono- and dipeptides. The most interesting observations relate to the question of intramolecular hydrogen bonding and chirality organization around the metallocene backbone, which acts as a template for the organization of the peptide strands particularly in the disubstituted derivatives **4**.

In the solid state, intra- and intermolecular hydrogen bonds are of similar strength and hence other factors may dominate the molecular conformation. In solution, however, intramolecular hydrogen bonding is strongly favoured and the same pattern seems to emerge for most compounds studied so far, including the ones in this study (''Herrick conformation''), namely a symmetrical 1,2′ orientation of the amide substitutents on the Cp ring with two strong intramolecular hydrogen bonds. NMR, IR and CD spectroscopic investigations all support this assumption.

The ready preparation of ferrocene peptides with functional side chains opens the way to further derivatization. In particular, thiol derivatives provide easy access to further conjugation, for example with fluorecent dyes, by reaction with maleiimide or iodo acetic acid reagents. Preliminary results on the sulfur deprotection chemistry suggest that free thiol groups should become available for further derivatization, although careful control of the reaction conditions is certainly required. Work along those lines is in progress in our laboratory.

Acknowledgements

The authors are grateful to H. Rudy (MS and elemental analysis) and T. Zimmermann (NMR) for technical assistance. Dr. M. Enders is thanked for running 2D NMR spectra of our samples. Mrs. Berangère Macabeo (ERASMUS program) and Mrs. Shani Treves (twin city student exchange program with Rehovot, Israel) helped with the synthesis and measurements. Dr. S. Kirin and Prof. Dr. H.-B. Kraatz have contributed through insightful discussions. Financial support from the Fond der Chemischen Industrie and the Deutsche Forschungsgemeinschaft (DFG) within the Sonderforschungsbereich 623 is also gratefully acknowledged.

References

[1] K. Severin, R. Bergs, W. Beck, Angew. Chem. 110 (1998) 1722; Angew. Chem., Int. Ed. Engl. 37 (1998) 1634–1654.
[2] P. Saweczko, H.-B. Kraatz, Coord. Chem. Rev. 190–192 (1999) 185.
[3] Y. Xu, H.-B. Kraatz, Tetrahedron Lett. 42 (2001) 2601.
[4] H.-B. Kraatz, M. Galka, Met. Ions Biol. Syst. 38 (2001) 385.
[5] K. Plumb, H.-B. Kraatz, Bioconjugate Chem. 14 (2003) 601.
[6] P.D. Beer, P.A. Gale, Coord. Chem. Rev. 185–186 (1999) 3.
[7] P.D. Beer, P.A. Gale, Angew. Chem., Int. Ed. Engl. 40 (2001) 486; Angew. Chem. 113 (2001) 502–532.
[8] R.S. Herrick, R.M. Jarret, T.P. Curran, D.R. Dragoli, M.B. Flaherty, S.E. Lindyberg, R.A. Slate, L.C. Thornton, Tetrahedron Lett. 37 (1996) 5289.
[9] T. Moriuchi, T. Hirao, Chem. Soc. Rev. (2004) 294.
[10] D.R. van Staveren, T. Weyhermüller, N. Metzler-Nolte, J. Chem. Soc., Dalton Trans. (2003) 210.
[11] I.R. Butler, S.C. Quayle, J. Organomet. Chem. 552 (1998) 63.
[12] T. Okamura, K. Sakauye, N. Ueyama, A. Nakamura, Inorg. Chem. 37 (1998) 6731.
[13] K. Heinze, M. Schlenker, Eur. J. Inorg. Chem. (2004) 2974.
[14] L. Barisic, V. Rapic, V. Kovac, Croat. Chem. Acta 75 (2002) 199.
[15] L. Barisic, M. Dropucic, V. Rapic, H. Pritzkow, S. Kirin, N. Metzler-Nolte, J. Chem. Soc., Chem. Commun. (2004) 2004.
[16] A. Nomoto, T. Moriuchi, S. Yamazaki, A. Ogawa, T. Hirao, J. Chem. Soc., Chem. Commun. (1998) 1963.
[17] T. Moriuchi, K. Yoshida, T. Hirao, J. Organomet. Chem. 668 (2003) 31.
[18] T. Moriuchi, K. Yoshida, T. Hirao, J. Organomet. Chem. 637–639 (2001) 75.
[19] T. Moriuchi, K. Yoshida, T. Hirao, Organometallics 20 (2001) 3101.
[20] T. Moriuchi, A. Nomoto, K. Yoshida, T. Hirao, Organometallics 20 (2001) 1008.
[21] T. Moriuchi, A. Nomoto, K. Yoshida, A. Ogawa, T. Hirao, J. Am. Chem. Soc. 123 (2001) 68.
[22] T. Moriuchi, A. Nomoto, K. Yoshida, T. Hirao, J. Organomet. Chem. 589 (1999) 50.
[23] H.-B. Kraatz, J. Lusztyk, G.D. Enright, Inorg. Chem. 36 (1997) 2400.
[24] L. Lin, A. Berces, H.-B. Kraatz, J. Organomet. Chem. 556 (1998) 11.
[25] M.V. Baker, H.-B. Kraatz, J.W. Quail, New J. Chem. 25 (2001) 427.
[26] Y. Xu, P. Saweczko, H.-B. Kraatz, J. Organomet. Chem. 637–639 (2001) 335.
[27] M. Oberhoff, L. Duda, J. Karl, R. Mohr, G. Erker, R. Fröhlich, M. Grehl, Organometallics 15 (1996) 4005.
[28] A.S. Georgopoulou, D.M.P. Mingos, A.J.P. White, D.J. Williams, B.R. Horrocks, A. Houlton, J. Chem. Soc., Dalton Trans. (2000) 2969.
[29] D.R. van Staveren, N. Metzler-Nolte, Chem. Rev. (2004) in print.
[30] SHELXTL, Siemens Analytical X-ray Instruments, Inc, 1994.
[31] G.M. Sheldrick, SHELX97, University of Göttingen, Göttingen, Germany, 1997.
[32] A. Hess, J. Sehnert, T. Weyhermüller, N. Metzler-Nolte, Inorg. Chem. 39 (2000) 5437.
[33] D.R. van Staveren, T. Weyhermüller, N. Metzler-Nolte, Organometallics 19 (2000) 3730.
[34] S.H. Gellman, G.P. Dado, G.-B. Liang, B.R. Adams, J. Am. Chem. Soc. 113 (1991) 1164.
[35] G.-B. Liang, G.P. Dado, S.H. Gellman, J. Am. Chem. Soc. 113 (1991) 3994.
[36] G.C.K. Roberts, NMR of Macromolecules – A Practical Approach, Oxford University Press, Oxford, 1993.
[37] A. Rodger, B. Nordén, Circular Dichroism and Linear Dichroism, Oxford University Press, Oxford, 1997.
[38] H.-B. Kraatz, Macromol. Symp. 196 (2003) 39.
[39] I. Bediako-Amoa, R. Silerova, H.-B. Kraatz, Chem. Commun. (2002) 2430.
[40] Q.-W. Han, X.-Q. Zhu, X.-B. Hu, J.-P. Cheng, Chem. J. Chin. Univ. 23 (2002) 2076.
[41] H. Huang, L. Mu, J. He, J.-P. Cheng, J. Org. Chem. 68 (2003) 7605.
[42] C.N. Kirsten, T.H. Schrader, J. Am. Chem. Soc. 119 (1997) 12061.
[43] H.-B. Kraatz, Personal communication, 2004.